Noise control of subsonic cavity flows using passive receptive channels

A. Das Gupta and S. Roy
Applied Physics Research Group, University of Florida, Gainesville, FL, 32611

We introduce a passive receptive channel in an open rectangular cavity to reduce the acoustic tones generated due to coherent shear layer impingement. The rectangular channel is placed at the trailing edge of the cavity. It is easy to implement and is a passive controller that responds to the flow for a wide range of operating conditions. Different orientation for the rectangular channel has been numerically tested at Mach 0.1, 0.3 and 0.5. Numerical results using unsteady three-dimensional large eddy simulation showed that the channel reduced the coherence of the shear layer which caused the acoustic suppression resulting in a reduction of the sound pressure levels for all three Mach numbers tested. Specifically, the acoustic suppression of 10 dB was obtained for Mach 0.3 flow with a 71.56° channel. The channel can be useful in noise reduction for various applications including weapons bay, landing gear and branched piping systems.

I. INTRODUCTION

Flow over an open cavity generates acoustic tones caused by pressure oscillations generated from impinging shear layers. Free shear layers in an open cavity become unstable and create large vortical structures, which impinge on the trailing edge and produce periodic acoustic waves. These waves propagate upstream and when it reaches the leading edge of the cavity, it perturbs the shear layer causing an instability. This effect of unstable shear layers is governed by Kelvin Helmholtz instability mechanism. Thus the downstream travelling vortices and the upstream travelling acoustic waves form a closed path, which leads to resonance in the open cavity. Figure 1 shows some of the important parameters governing resonant cavity flows [1], including incoming turbulent boundary layer thickness, disturbance wavelength λ, cavity length L, and cavity depth D. It also shows travelling vortices and the feedback from the trailing edge.

Acoustic resonance in cavities has a variety of applications [2-4]. Its effects can be detrimental or beneficial depending on the usage. On one hand it is beneficial in generating music in wind instruments and whistles but on the other hand it is detrimental for applications such as landing gear and weapons bay in aircrafts where it can damage the fragile parts [3, 4]. Resonant cavities are also found in branched and corrugated piping systems where one can get severe noise problems, like the whistling phenomena [2]. In this paper, we introduce a passive flow control method to reduce the detrimental effects of acoustic waves in an open cavity.

In general, flow control methods can be classified into active and passive methods. Active control methods use external energy/momentum source to control the flow like mechanical or electrical input while passive control is done via geometric modifications. Examples of passive control methods include rigid fences, spoilers, ramps and passive bleed systems. The widely used passive control method is spoiler which has been implemented on aircrafts such as B-47, F-111 and B-1. Heller and Bliss [3] used large vortex generator tabs mounted at the leading edge to suppress oscillations. They also studied a combination of leading edge spoiler and slant trailing edge. However, extensive study on trailing edge geometric modification has not been explored. Rossiter [4] used a guillotine-type spoiler at the leading edge to alter the boundary layer thickness. Shaw [5] explored sloped trailing edge ramp, leading edge spoilers and airfoils to reduce the oscillations. Sarno and Franke [6] employed leading edge ramps. Application of rods at the leading edge has been very promising in reducing the cavity tones. The first successful test using rods in cross flow was performed by Maines et. al. [7] and they showed a reduction of 20 dB for Mach 1.2 flow. Ukeiley et.al [8] used a combination of leading edge fence and rods to suppress the cavity oscillations.

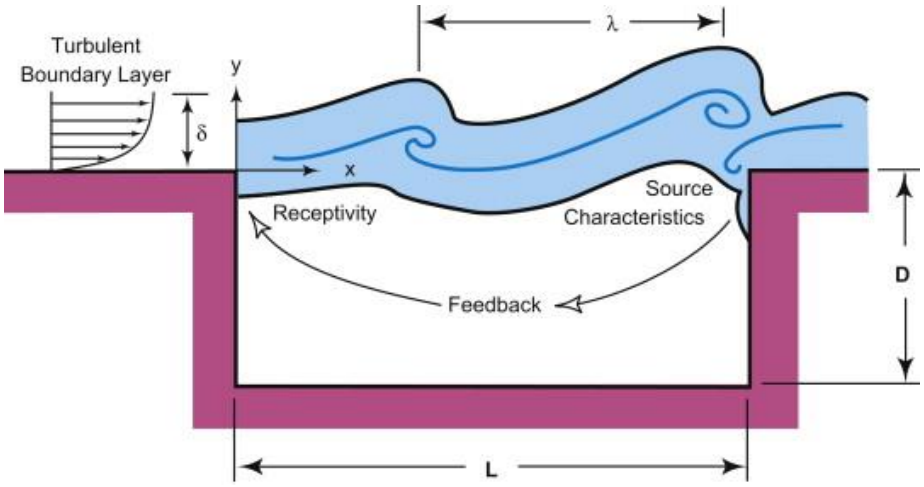

FIG.1. Shear flow characteristics in an open cavity[1]

Active control can be classified as closed loop and open loop. In the closed loop active control method, the flow conditions are directly sensed or estimated and a feedback system is employed to change the control signal input accordingly. Most of these methods rely on changing the shear layer instability characteristics, the shear layer attachment location or the coherent nature of the shear layer. Active control methods like leading edge steady/pulsed mass injection to control the cavity tones have become very popular.

Both active and passive control methods have been investigated using physical and numerical experiments. Experimental work on subsonic open cavity flow was conducted by Murray et. al. [9] for different Mach numbers. Numerical study has been done on deep [10] and shallow cavity [11] at high subsonic speed using large eddy simulation for a better estimation of pressure peaks. Stanek [12] used resonating cylindrical rods for acoustic suppression. Debiassy and Samimy [13] presented a logic based active closed loop control to selectively reduce the sound pressure levels. They used a leading edge pulsed blower and conducted experiments for a range of Mach numbers. MacManus and Doran [14] studied the effect of introducing a leading edge step on the resonant frequencies for transonic speeds. Different passive control techniques for transonic flow was studied by Lawson and Barakos [15] and they showed that a rear sloped wall gives the largest noise reduction in the front half of the cavity compared to leading edge spoilers. More examples of different passive and active control methods can be found in Cattafesta et.al [1]. However, these methods have their own set of limitations. For example, passive control methods do not work for a wide range of Mach numbers [16]. Active control methods require complicated circuitry and additional subsystems. Open loop methods are also mostly design specific.

In this paper, we introduce a receptive channel in the trailing edge as a passive control mechanism of the acoustic tones that requires minimal geometric modification of the standard cavity. The idea is to connect the fluid between the high and low pressure regions around the trailing edge, which in turn should reduce the pressure oscillation amplitudes and thus influence the noise levels. We study a range of Mach numbers for various channel orientations to show the effect of such geometric modifications. Our paper is organized in the following manner. Section 2 will describe the geometry and simulation details for our problem. Section 3 will present three-dimensional simulation results for the flowfield as well as the acoustic data. Finally, section 4 will derive a brief conclusion and suggest future research pathways.

II. CAVITY MODEL

The baseline cavity model shown in Figure 2 is a standard open rectangular cavity. All relevant dimensions are given in Table I. The L/D ratio (x_c / y_c) is maintained at four throughout our study.

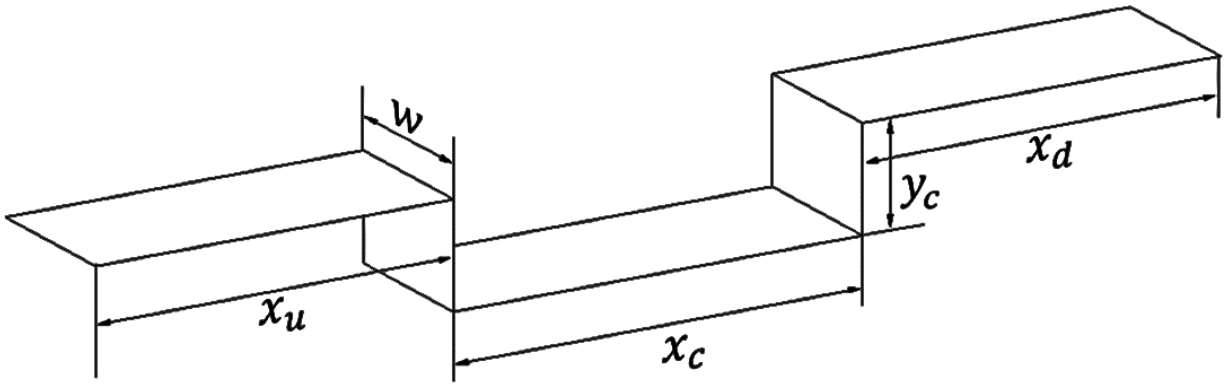

FIG.2. Open rectangular cavity schematic

Table 1. Dimensions of the cavity

Name	Symbol	Length (m)
Upstream length	x_u	0.889
Downstream length	x_d	0.889
Cavity length	x_c	1.016
Cavity height	y_c	0.254
Cavity width	w	0.381

The domain is divided into 4 blocks as shown in Figure 3 to obtain a structured non uniform mesh for better resolution of the free shear layer and its neighboring regions. Mesh resolution study for the cavity is performed using a coarse mesh and a fine mesh. Table II gives the mesh details. Figure 4 shows that the selected mesh for the coarse grid is sufficient enough to resolve the flowfield for which the acoustic data does not change significantly.

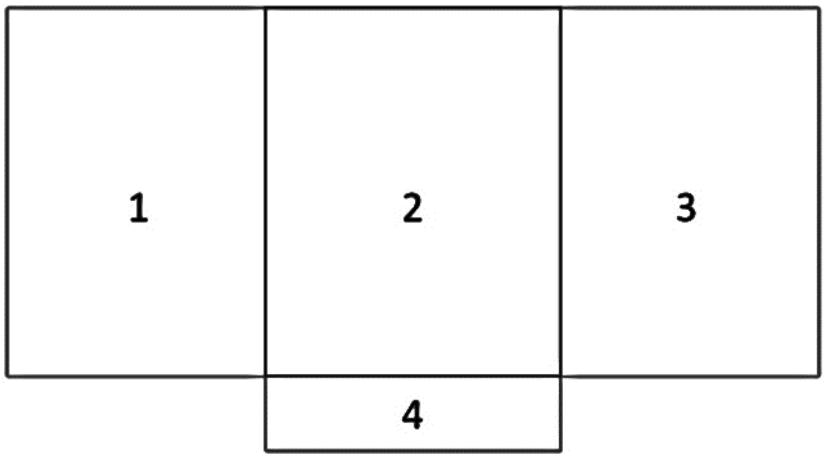

FIG.3. Two dimensional view of the blocking and their respective block numbers

The passive receptive channel shown in Figure 5 is placed on the trailing edge of the cavity, and only the angle of the channel is varied to get different configurations. The dimensions for the channel are provided in Table III. The meshing of the channel is done using unstructured mesh which contains quadrilateral as well as triangular

elements. The total number of elements in the channel is adjusted to 100,000 elements, while maintaining the same minimum y^+ as in the upstream region.

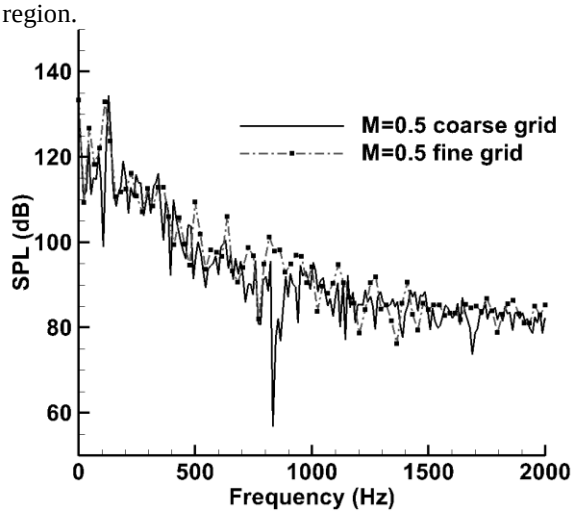

FIG.4. Grid resolution study

Table 2. Mesh details for the cavity

	Mesh (coarse)		**Mesh (fine)**	
Block	**Elements**	**Min y^+**	**Elements**	**Min y^+**
1	$60 \times 60 \times 30$	$1.0e-2$	$60 \times 80 \times 30$	$1.0e-3$
2	$120 \times 60 \times 30$		$200 \times 80 \times 30$	
3	$30 \times 60 \times 30$		$30 \times 80 \times 30$	
4	$120 \times 100 \times 30$		$200 \times 150 \times 30$	

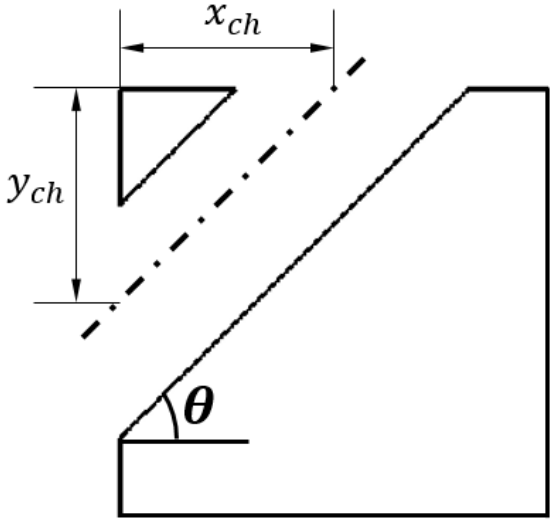

FIG.5. Trailing edge channel schematic

The length x_{ch} is the distance from trailing edge to the center line of the channel. The angle θ, which the channel makes with the horizontal is varied from 18.43° to 71.56° which makes x_{ch} vary from 0.00838 m to 0.0762 m. The height of the channel y_{ch} is kept constant at 0.0254 m. Hereafter, we shall call the 18.43° case as case I, 45° as case II and 71.56° as case III.

Table 3. Channel dimensions

Symbol	Case I	Case II	Case III
x_{ch}	0.0762 m	0.0254 m	0.00838 m
y_{ch}	0.0254 m	0.0254 m	0.0254 m
θ	18.43°	45°	71.56°

The numerical simulation is performed in Ansys Fluent® 14.5 using the large eddy simulation (LES) with Smagorinsky-Lilly model as the sub-grid scale model. The free stream conditions are for Mach 0.1, 0.3 or 0.5 at a temperature of 225 K and ambient pressure of 24.95 kPa. No slip and adiabatic conditions are applied to the cavity walls. The side faces have periodic boundary conditions. Farfield conditions are used for the top boundary and the outflow is kept as non-reflecting pressure outlet. The acoustic part is solved using the Ffowcs Williams and Hawkings model [17]. The model is used to predict acoustic pressure at three different receiver locations shown in Figure 6 and are placed on the center z-plane, 1 mm from the wall surface. All simulations are run till the sound pressure levels stop changing. The next section will discuss all the results obtained for the flow field and the acoustic data for the cavity.

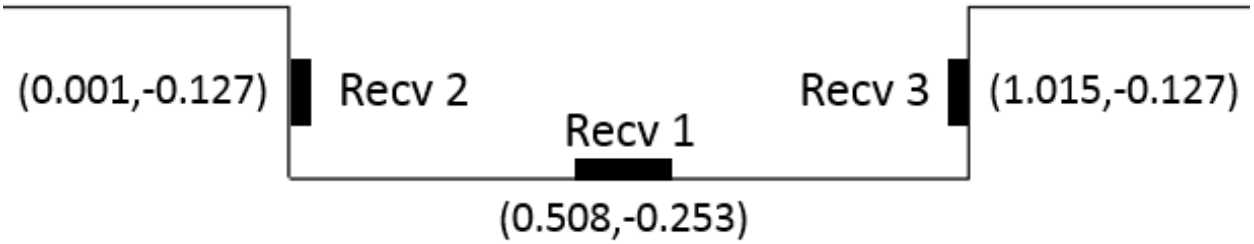

FIG. 6. Schematic of the receiver location

III. RESULTS

We have conducted the flow simulation and acoustic analysis for the cases enlisted in Table IV. For brevity, we present flow simulation results only for M = 0.3 cases. However, acoustic data is presented for all the cases shown in Table IV. Since Fluent has been validated as a flow code for variety of problems [18, 19], as well as for open rectangular cavities [20, 21], therefore no validation results are presented for the flow field.

Table 4. Simulation cases

Mach Number	0.1	0.3	0.5
Cases	Baseline, Case II	Baseline, Case I, Case II, Case III	Baseline, Case II

A. Flow field Analysis

As mentioned in the previous section the channel geometry has been tested for three different Mach numbers and the angle of the channel has also been varied to understand its effects. The results in this section are for M = 0.3.

Figure 7 shows the time averaged pressure contours for the mid z – plane and we can clearly see the high pressure and low pressure regions at the trailing edge of the cavity. The contours shows time averaged gauge pressure varying from -1.1 to 1.1 kPa (higher values are redder).

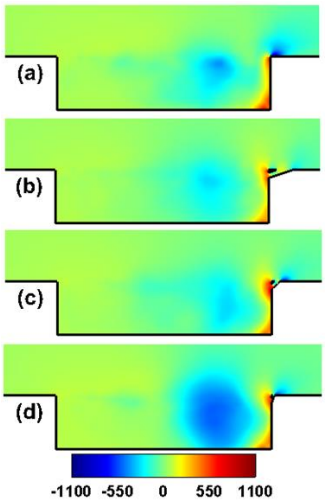

FIG.7. Time average pressure contour at the center z plane (a) Baseline (b) 18.43° (case I) channel (c) 45° (case II) channel (d) 71.56° (case III) channel

The spanwise variation of the time averaged pressure field is shown in Figure 8. We can see alternate positive and negative pressure in the cavity, which indicates the presence of acoustic waves as well as the three dimensional nature of the flow. As the flow approaches the trailing edge these pressure oscillations become significant and create acoustic waves which propagate upstream. We understand that one way of reducing the amplitude of the acoustic tones is to reduce the amplitude of the pressure fluctuations. To do that we have introduced the channel at the trailing edge so that the fluid has a passage between the high and low pressure regions, which in turn would reduce the pressure oscillation amplitude.

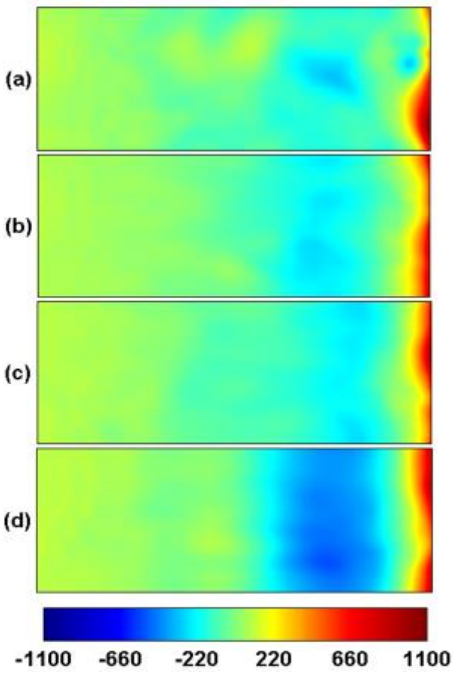

FIG.8. Time average pressure contour at the y = -0.01 plane (a) Baseline (b) 18.43° (case I) channel (c) 45° (case II) channel (d) 71.56° (case III) channel

Both Figure 7 and Figure 8 show the effect of the passive receptive channel on the cavity flow. The high pressure region close to the cavity trailing edge from which the acoustic waves emanate has been diffused and spread over the entire span of the cavity. The peak values of pressure are reduced from 1.3 kPa for the baseline case to 700 kPa for case I, 600 kPa for case II and 1000 kPa for case III. Carefully observing Figure 7, we find the high pressure region close to the cavity bottom wall is also suppressed. In order to understand the influence of the channel on shear and vorticity we plot the Q criterion in Figure 9, evaluated using the following equation.

$$Q = \frac{1}{2}\left\{\left(\omega_x{}^2 + \omega_y{}^2 + \omega_z{}^2\right) - \left(\tau_{xx}{}^2 + \tau_{xy}{}^2 + \tau_{xz}{}^2 + \tau_{yx}{}^2 + \tau_{yy}{}^2 + \tau_{yz}{}^2 + \tau_{zx}{}^2 + \tau_{zy}{}^2 + \tau_{zz}{}^2\right)\right\} \quad (1)$$

Based on the Q criterion it is evident that the introduction of channel reduces the regions of shear (blue region) compared to the large scale vortices (red region).

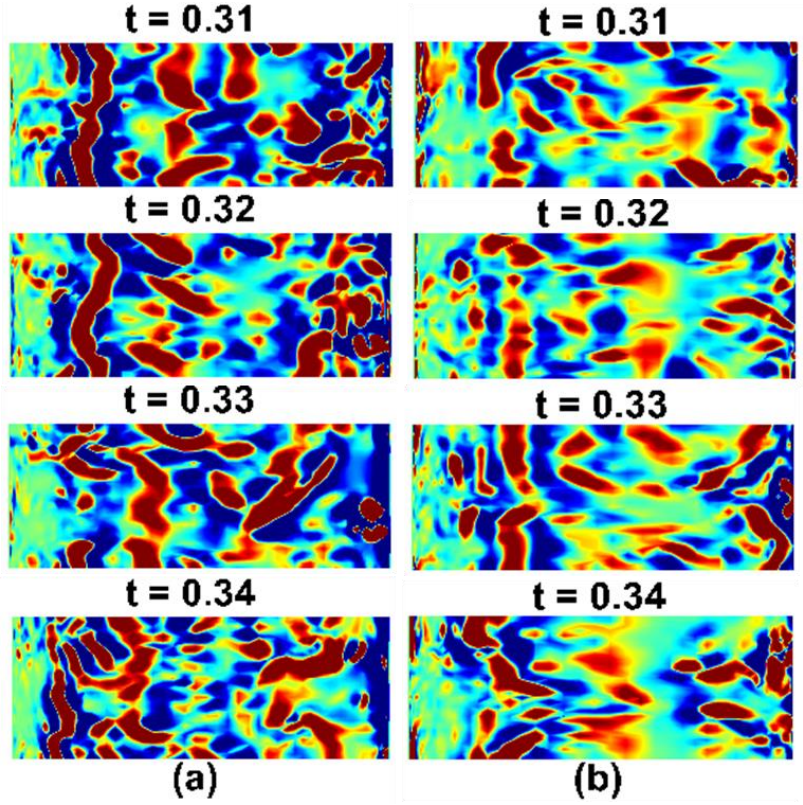

FIG.9. Instantaneous Q criterion contour for y = -0.01m plane at different times (a) Baseline (b) 45° (case II) channel (blue is -1e-5 and red is +1e-5)

The iso-surfaces of Q criterion are shown in Figure 10. The yellow regions correspond to the rotational component dominating the shear and the blue regions correspond to the shear dominating the rotational component. We can see that, as the angle gets steeper the free shear layer gets less coherent. Thus we obtain the lowest sound pressure levels for case III. The streamwise velocity contours depicted in Figure 11 show that shear layer is being shifted downwards into the cavity from the trailing edge. This can be another factor for the reduction in sound pressure levels. The contours have been only shown up to 90m/s to have a better visualization of the free shear layer. Case III geometry has been used to obtain the acoustic data for M = 0.1 and M = 0.3. The next section will show the acoustic data for all the cases.

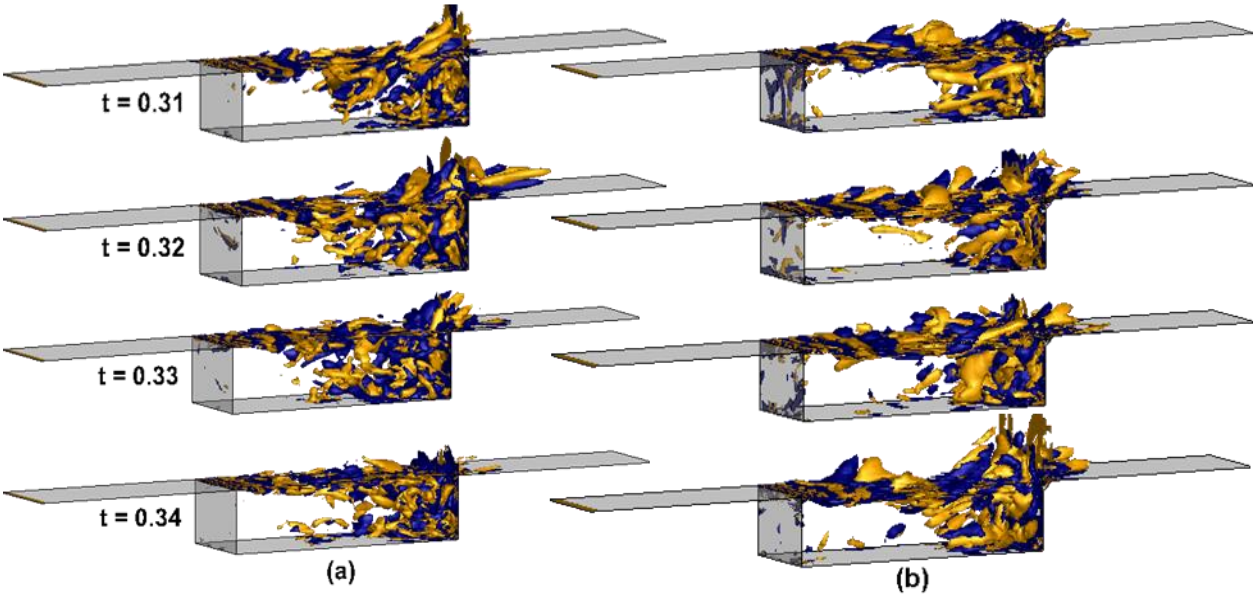

FIG.10. Instantaneous Q criterion iso-surface at t = 0.3 (a) Baseline (b) 18.43° (case I) channel (c) 45° (case II) channel (d) 71.56° (case III) channel (blue is -1e-5 and yellow is +1e-5)

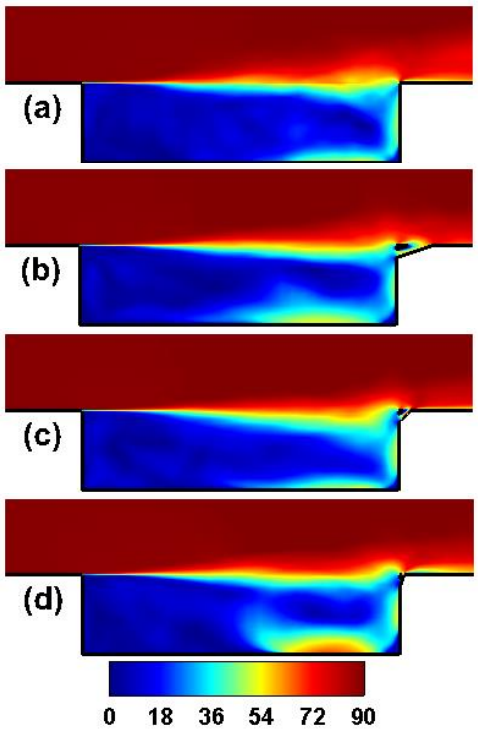

FIG.11. Time average velocity magnitude contour for center z plane (a) Baseline (b) 18.43° (case I) channel (c) 45° (case II) channel (d) 71.56° (case III) channel

B. Acoustic Analysis

To validate the acoustic data of our simulation, the frequencies of different modes are compared to the resonant frequencies predicted by Rossiter [4]. The comparison is shown in Figure 12. The Rossiter frequencies [4] are obtained the following equation.

$$f_n = \frac{U_\infty}{L}\frac{n-\phi}{M_\infty\left\{1+\left[(\gamma-1)/2\right]M_\infty{}^2\right\}^{-\frac{1}{2}}+\frac{1}{k}} \tag{2}$$

In *Equation* (2), different integer mode numbers are given by *n*, *L* is the streamwise cavity length, U_∞ and M_∞ are the freestream velocity and Mach number, f_n is the Rossiter frequency, ϕ is the phase lag between the downstream travelling Kelvin – Helmholtz Instabilities and the upstream travelling acoustic waves and *k* denotes the ratio of convective speed of the shear layer instabilities and the freestream velocity. The values of ϕ = 0.25 and *k* = 0.66 are used to obtain Figure 12. Most of the modes are captured accurately.

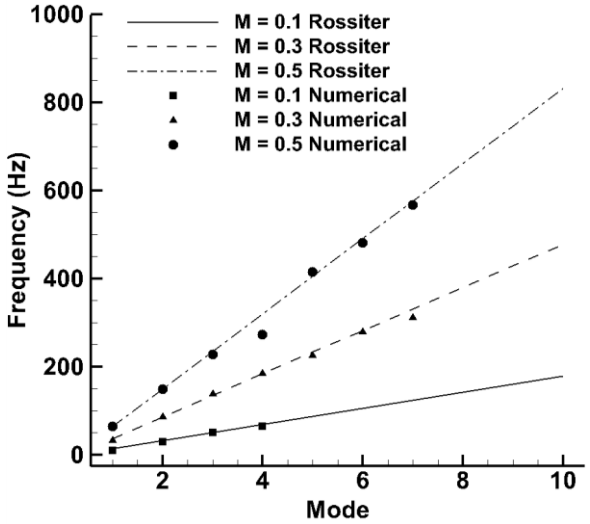

FIG.12. Comparison of the Resonant Frequencies obtained from simulation with Rossiter frequencies at different Mach numbers

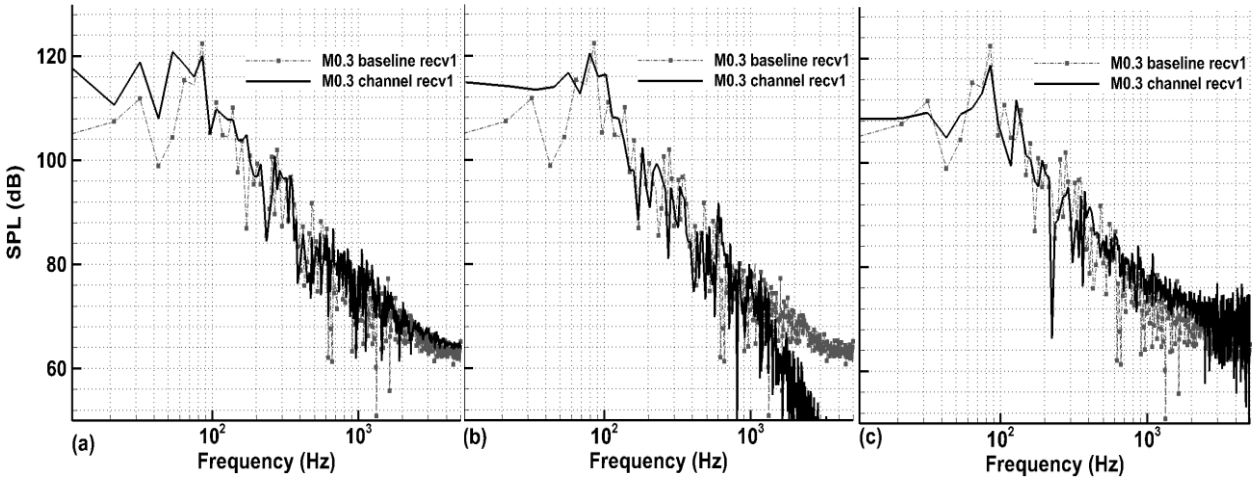

FIG.13. Sound spectrum for M = 0.3at receiver 1 (a) case I (b) case II (c) case III

Looking at the sound pressure level spectrum (ref 20μPa) in Figures 13-15 show that introducing the channel suppresses the sound pressure level for a wide range of frequencies. However the maximum suppression varies from 2 dB up to 10 dB depending on the receiver location. The best reduction is seen at receiver 3 location. There are some peaking and peak splitting observed which can have adverse effects. However looking at Figure 15(c) we see that almost all the peaking and peak splitting have been reduced. The effect of channel on sound pressure levels at different

locations shows that for *case I* the effect is insignificant. However for *case II* and *case III* the effects are significant. This can be attributed to the fact that for case I the channel outlet distance x_{ch} is maximum, due to which the low and high pressure regions at the trailing edge are not well connected.

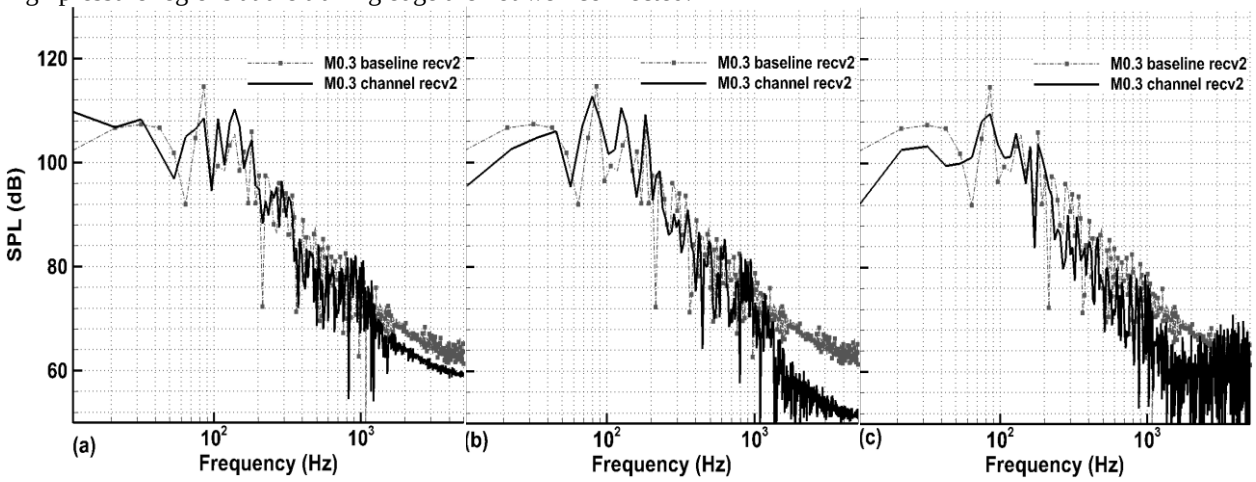

FIG.14. Sound spectrum for M = 0.3 at receiver 2 (a) case I (b) case II (c) case III

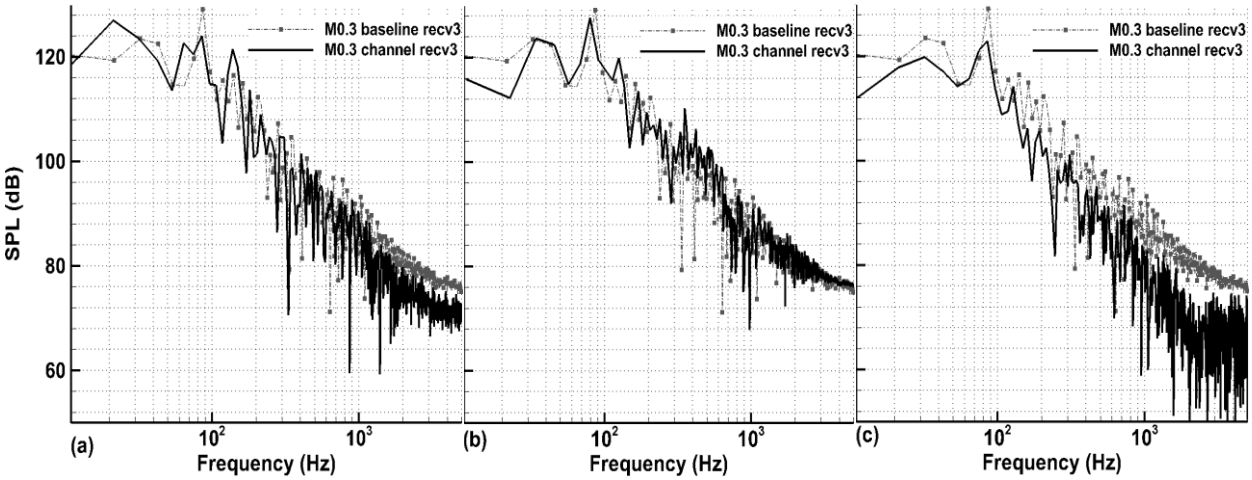

FIG.15. Sound spectrum for M = 0.3 at receiver 3 (a) case I (b) case II (c) case III

Figure 16 shows the effect of a 45° channel at Mach 0.1, 0.3 and 0.5. For M = 0.1 the numerical solution gives multiple modes along with the Rossiter modes. This is due to the high time stepping used to capture the lower frequencies in the cavity. However this is not observed for the channel case or any other case. We also find that the peak power spectral density is reduced in all the cases.

IV. CONCLUSION

Introduction of a passive receptive channel placed at the trailing edge shows an appreciable effect on the acoustic tones in the cavity. The channel is found to change the coherence of the shear layer and also the impingement location. Three different angles of the channel have been explored at various flow speeds. Sound pressure levels are reduced in all the cases. The best reduction for M = 0.3 is obtained for the 71.56° channel at the receiver closest to the trailing edge where a 10 dB reduction is observed for majority of the frequency spectrum. For frequencies higher than 1 kHz most of the cases show 5 to 15dB reduction. The power spectral density is suppressed by 25 – 45% for Mach numbers ranging from 0.1 – 0.5. These encouraging trends underscore a need for extending this study in the transonic and supersonic regime where the effect of channel geometry should be significant. The use of channel along with

other passive or active devices should also be investigated to get better suppression of acoustic tones. Conducting experiments for this new passive control channel will give useful insights and validate our predictions.

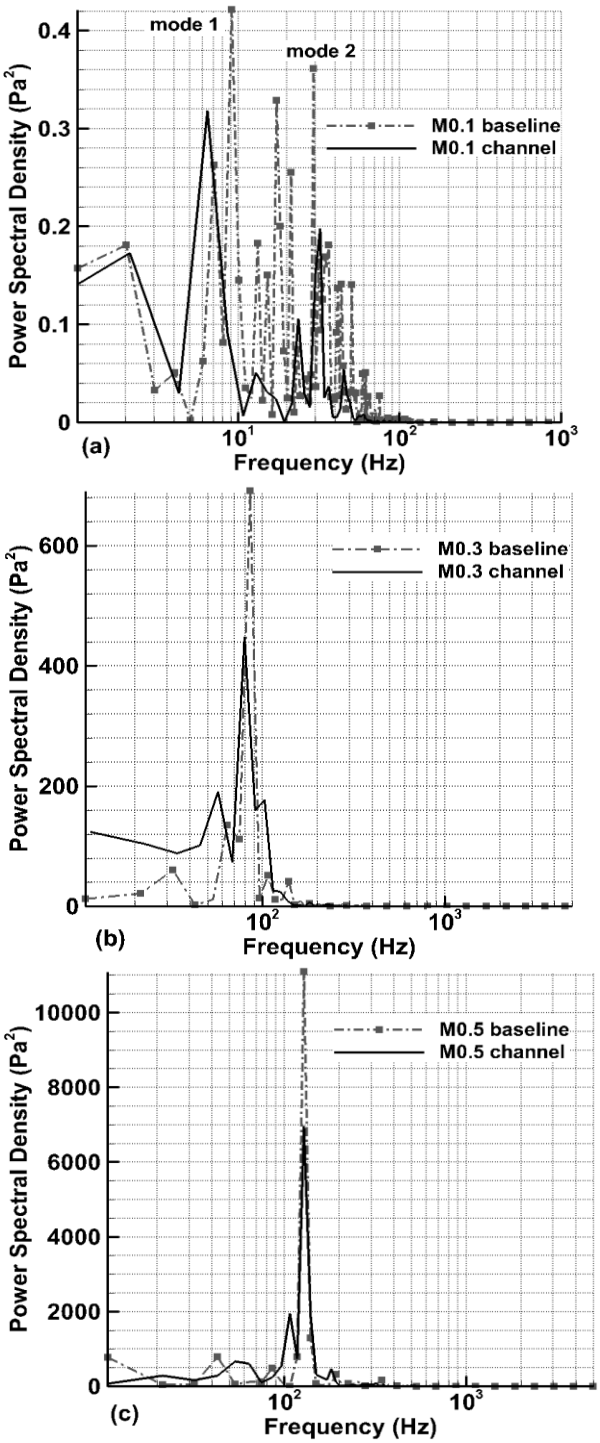

FIG.16. Power spectrum at receiver 1 for 45° channel (a) M = 0.1 (b) M = 0.3 (c) M = 0.5

References

[1]Cattafesta,L., Song, Q., Williams, D.R., Rowley, C.W., and Alvi, F.S., "Active control of flow-induced cavity oscillations," *Progress in Aerospace Sciences,* pp. 479-502, 2008.

[2]Nakiboğlu, G., Belfroid, S.P., Willems, J.F., and Hirschberg, A. "Whistling behavior of periodic systems: Corrugated pipes and multiple," *International Journal of Mechanical Sciences,* pp. Vol 52, 1458-1470, 2010.

[3]Heller, H.H., and Bliss, D.B., "Aerodynamically Induced Pressure Oscillations In Cavities - Physical Mechanisms and Suppression Concepts," *AFFDL-TR-74-133,* 1975.

[4]Rossiter, J.E., "Wind Tunnel Experiments On the Flow Over Rectangular Cavities for Subsonic and Transonic Speeds," RAE TR 64037 Aeronautical Research Council, 1964.

[5]Shaw, L.L., "Suppression of aerodynamically induced cavity oscillations," AFFDL-TR-79-3119, Nov 1979

[6]Sarno, R.L., and Franke, M.E., "Suppression of Flow-Induced Pressure Oscillations in Cavities," *Journal of Aircraft,* pp. 90-96, 1994.

[7]Maines, B., Robarge, J., Welterlen, T.J., and Smith, B.R., "Weapons Bay Acoustic Suppression From A Rod In Crossflow," in *AIAA Aerospace Sciences Meeting*, 2001.

[8]Ukeiley, L.S., Ponton, M.K., Seiner J.S., and Jansen, B., "Suppression of Pressure Loads in Cavity Flows," *AIAA journal,* vol. 42, no. 1, pp. 70-79, 2004.

[9] Nathan Murray, Erik Sällström, and Lawrence Ukeiley, " Properties of subsonic open cavity flow fields," *Physics of Fluids,* vol. 21, pp. 095103-16, 2009.

[10]Larcheveque, L., Sagaut, P., Mary, I., and Labbe, O., "Large-eddy simulation of a compressible flow past a deep cavity," *Physics of Fluids,* vol. 15, pp. 193-210, Jan 2003.

[11]Larcheveque, L., Sagaut, P., Le T.H., and Comte, P., "Large-eddy simulation of a compressible flow in a three-dimensional open cavity at high Reynolds number," *Journal of Fluid Mechanics,* vol. vol 516, pp. 265-301, 2004.

[12]Stanek, M.J., "A Numerical Study of the Effect of Frequency of Pulsed Flow Control Applied to a Rectangular Cavity in Supersonic Crossflow," Unicersity of Cincinnati, 2005.

[13]Debiasi M., and Samimy, M,, "Logic-Based Active Control of Subsonic Cavity Flow Resonance," *AIAA journal,* pp. Vol. 42, No. 9, 1901-1909, 2004.

[14]MacManus, D.G., and Doran, D.S., "Passive Control of Transonic Cavity," *Journal of Fluids Engineering,* pp. Vol. 30, 064501-1-4, 2008.

[15]Lawson, S.J., and Barakos, G.N., "Assessment of Passive Flow Control for Transonic Cavity Flow Using Detached-Eddy Simulation," *Journal of Aircraft,* pp. Vol. 46, No. 3, 1009-1029, 2009.

[16]Shaw, L.L., and Shimovetz, R.M., "Weapons Bay Acoustic Environment", Symposium on the Impact of Acoustic Loads on Aircraft Structures, AGARD-CP-549, Lillehammer, Norway, May 1994.

[17]Williams, J.E.F., and Hawkings, D.L., "Sound Generation by Turbulence and Surfaces in arbitrary motion," *Mathematical and Physical Sciences,* pp. Vol. 264, 321-342, 1969.

[18]Catalano, P., Wang, M., Iaccarino, G., and Moin, P., "Numerical simulation of the flow around a circular cylinder at high Reynolds numbers," *International Journal of Heat and Fluid Flow,* vol. 24, no. 4, pp. 463-469, Aug 2003.

[19]Luo, X., Hinton, J., Liew, T., and Tan, K., "LES modelling of flow in a simple airway model," *Medical Engineering and Physics,* vol. 26, no. 5, pp. 403-413, June 2004.

[20] Ritchie, S.A., Lawson, N.J., and Knowles, K., "An experimental and numerical investigation of an open transonic cavity." *21st Applied Aerodynamics Conference*, AIAA, Orlando, 2003.

[21]Ooi, A., Iaccarino, G., Durbin, P. and Behnia, M., "Reynolds averaged simulation of flow and heat transfer in ribbed ducts," *International Journal of Heat and Fluid Flow*, vol. 23, no. 6, pp. 750-757, Dec 2002.